Journal of Inorganic Biochemistry 190 (2019) 31–37

Contents lists available at ScienceDirect

Journal of Inorganic Biochemistry

journal homepage: www.elsevier.com/locate/jinorgbio

A new Cu(II)-*O*-Carvacrotinate complex: Synthesis, characterization and biological activity

Manas Sutradhar[a], Alexandra R. Fernandes[a,b], Fabiana Paradinha[b], Patricia Rijo[c], Catarina Garcia[c], Catarina Roma-Rodrigues[b], Armando J.L. Pombeiro[a], Adília Januário Charmier[a,d,*]

[a] CQE, Centro de Química Estrutural, Instituto Superior Técnico, Universidade de Lisboa, Av. Rovisco Pais, 1049-001 Lisboa, Portugal
[b] UCIBIO, Departamento Ciências da Vida, Faculdade de Ciências e Tecnologia, Universidade Nova de Lisboa, Campus Caparica, 2829-516, Portugal
[c] CBIOS, Universidade Lusófona de Humanidades e Tecnologias, Campo Grande 376, Lisbon 1749-024, Portugal
[d] DREAMS, Universidade Lusófona de Humanidades e Tecnologias, Campo Grande 376, Lisbon 1749-024, Portugal

ARTICLE INFO

Keywords:
Carvacrol
O-carvacrotinic acid
Cu(II) complex
Antiproliferative agent
Human tumor cell lines
Antimicrobial activity

ABSTRACT

Herein, we report the first example of the synthesis of a novel type of Cu(II) complex based on a natural product ligand derived from carvacrol. The copper(II) complex $[Cu(DCA)_2(EtOH)]_2 \cdot 2EtOH$ (**1**, HDCA=*O*-carvacrotinic acid) has been synthesized and characterized by elemental analysis, IR spectroscopy, ESI-MS and single crystal X-ray analysis. Complex **1** and the carvacrotinic acid (**2**, HDCA) have been studied towards their antimicrobial and antiproliferative activities. For both compounds the antimicrobial activity was assessed against a panel of Gram-positive and Gram-negative bacteria and yeasts. The microdilution method allowed the determination of their Minimum Inhibitory Concentration (MIC) and minimum bactericidal concentration (MBC). Interestingly, both compounds seem to be more effective on yeasts rather than bacteria especially against *C. albicans*. Regarding the antimicrobial properties, the compounds appear to present a bacteriostatic behaviour, rather than bactericide. The antiproliferative effect of complex **1**, *O*-carvacrotinic acid (HDCA) **2** and carvacrol (CA) **3** used as a reference to compare their antitumoral activity, was examined in 4 human tumor cell lines (ovarian carcinoma (A2780), colorectal carcinoma (HCT116), lung adenocarcinoma (A549) and breast adenocarcinoma (MCF7)) and in normal human primary fibroblasts. Complex **1** exhibits a moderate cytotoxic activity against ovarian carcinoma cells (A2780), with no cytotoxicity in normal primary human fibroblasts. The moderate cytotoxicity observed in A2780 cells was due to an increase of cell apoptosis.

1. Introduction

The antimicrobial activity of essential oils (EOs) and their components is attracting increasing attention in recent years [1–5]. The presence of phenolic compounds found in several EOs has been assigned the key component for their antimicrobial activity. For example, the efficiency of thyme, clove and oregano EOs is considered to originate from thymol, eugenol and carvacrol (CA) **3**, respectively. Carvacrol (5-isopropyl-2-methylphenol) **3** is a phenolic monoterpene present in the EO of the family Lamia-ceae, which includes the genera Origanum and Thymus, is considered one of the main components that exerts strong antimicrobial activity (can reach levels of 75%) [6,7], supported by its high specific activity compared to other EO components [8,9]. The inhibitory effect of the phenolic group in carvacrol **3** is supposed to result from the interactions with the cell membrane of microorganisms and is often correlated with the hydrophobicity of the compounds. Veldhuizen et al. studied the structural role of carvacrol **3** towards its antimicrobial activity by comparing other structurally similar compounds [10]. They showed that 2-amino-p-cymene has a similar membrane disruption and bacterial killing characteristics as carvacrol and the hydroxyl group of carvacrol itself is not essential for the antimicrobial activity. However, they observed a 3-fold lower activity for 2-amino-p-cymene as compared to carvacrol **3** which indicates a special mode of action of carvacrol **3** towards antimicrobial activity due to the presence of the hydroxyl group [10].

The effect of carvacrol **3** as an antiproliferative agent was also investigated by several groups [11–13]. Indeed recently, Dai and collaborators showed that carvacrol **3** suppressed proliferation and invasion of human oral squamous carcinoma cells via G1/S cell cycle arrest through downregulation of Cyclin D1 (CCND1) and Cyclin-dependent

* Corresponding author at: CQE, Centro de Química Estrutural, Instituto Superior Técnico, Universidade de Lisboa, Av. Rovisco Pais, 1049-001 Lisboa, Portugal.
E-mail addresses: ma.fernandes@fct.unl.pt (A.R. Fernandes), adilia.januario@ulusofona.pt (A.J. Charmier).

https://doi.org/10.1016/j.jinorgbio.2018.09.018
Received 23 May 2018; Received in revised form 26 September 2018; Accepted 27 September 2018
Available online 29 September 2018
0162-0134/

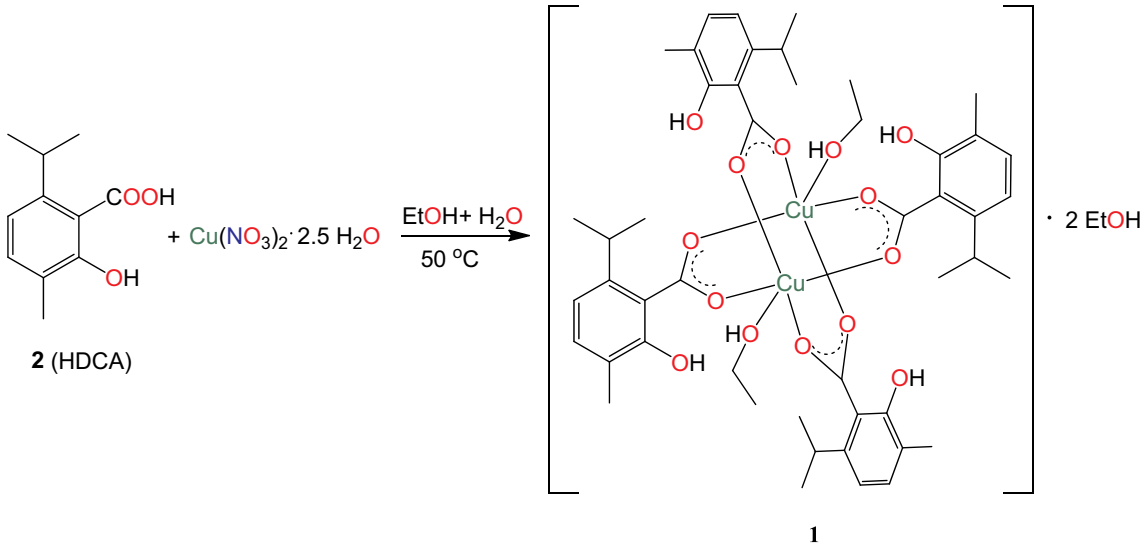

Scheme 1. Synthesis of complex **1**.

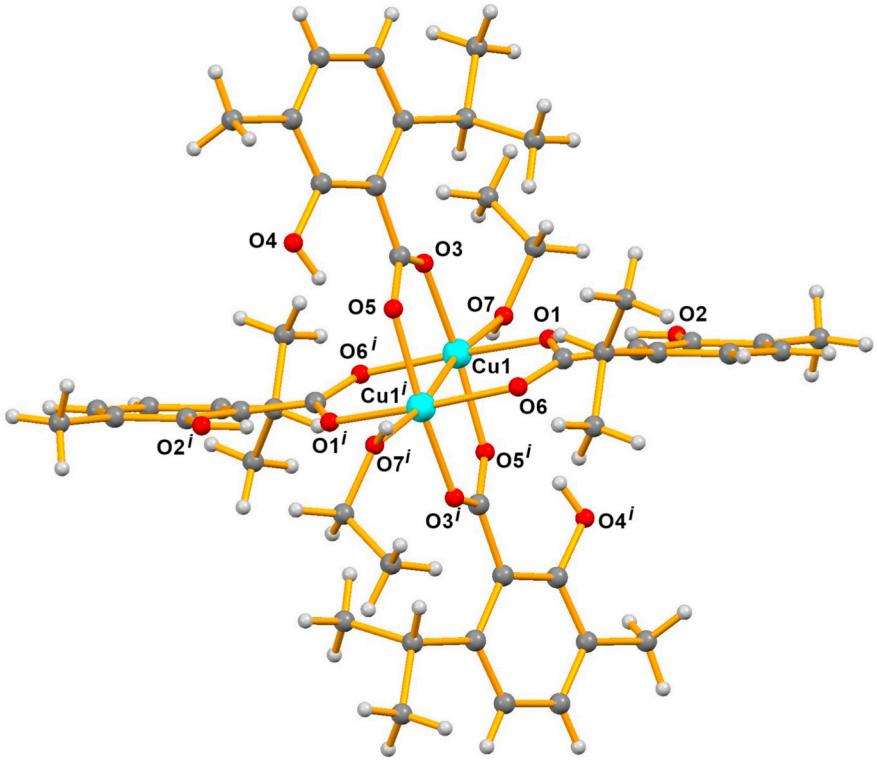

Fig. 1. Molecular structure of complex **1**. Solvent ethanol molecule omitted for clarity. *Symmetry code i = 1 − x,1 − y,1 − z.*

kinase 4 (CDK4) and upregulation of cyclin-dependent kinase inhibitor 1 (P21) and by blocking the phosphorylation of focal adhesion kinase (FAK) and reducing the expression of β-catenin, Zinc finger E-box-binding homeobox 1 (ZEB1), and metalloproteases (MMP) MMP-9 and MMP-2 [11]. Fan and collaborators [12] also showed that carvacrol **3** inhibited the proliferation of human colon cancer cell lines (HCT116 and LoVo) by G2/M cell cycle arrest and induced apoptotic cell death via the mitochondrial pathway and the mitogen-activated protein kinases (MAPK) and Phosphatidylinositol-4,5-bisphosphate 3-kinase/Protein Kinase B (PI3K/Akt) signaling pathways. The authors also demonstrate that carvacrol **3** reduced colorectal carcinoma cellular migration via the downregulation of matrix metalloprotease-2 (MMP-2) and MMP-9 expression [12]. The antimicrobial activity of carvacrol **3** is well known [14] and also other bioactivities [15]. The research on this compound has been undertaken to establish its biological properties towards its potential use, namely in clinical applications.

In the last years, intensive research has been focusing in using natural products or natural products derivatives for biological applications [16–20]. One of such example is the work of Ferrari and collaborators [21] were they studied the in vitro pharmacological activity of curcumin analogues and their copper complexes for the prevention and treatment of Alzheimer's disease. Yan and collaborators [22] also studied Curcumin-Cu(II) and -Zn(II) Complexes and their neuroprotective effects.

In this work, we synthesized the new copper(II) complex [Cu(DCA)$_2$(EtOH)]$_2$ ·2EtOH (**1**), derived from *O*-carvacrotinic acid (2-

Table 1
Crystal data and structure refinement details for complex **1**.

	1
Empirical formula	$C_{13}H_{19}Cu_{0.50}O_4$
Formula weight	271.05
Crystal system	Triclinic
Space group	$P\bar{1}$
Temperature/K	150 (2)
a/Å	10.6686 (5)
b/Å	11.5030 (5)
c/Å	11.9497 (5)
α/°	74.406 (2)
β/°	76.224 (2)
γ/°	77.188 (2)
V (Å^3)	1352.22 (11)
Z	4
D_{calc} (g cm^{-3})	1.331
μ(Mo Kα) (mm^{-1})	0.85
Rfls. collected/unique/observed	13,807/4953/4458
R_{int}	0.023
Final $R1$[a], w$R2$[b] ($I \geq 2\sigma$)	0.029, 0.071
Goodness-of-fit on F^2	1.04

[a] $R = \Sigma||F_o| - |F_c||/\Sigma|F_o|$.
[b] $wR(F^2) = [\Sigma w(|F_o|^2 - |F_c|^2)^2/\Sigma w|F_o|^4]^{1/2}$.

Table 2
Selected bond distances (Å) and angles (°) in complex **1**.

Cu1—O3			1.9521 (13)
Cu1—O6			1.9543 (13)
Cu1—O5			1.9662 (14)
Cu1—O1			1.9778 (13)
Cu1—O7			2.1162 (14)
Cu1—Cu1^i			2.5959 (4)
O3—Cu1—O6	89.07 (6)	O5—Cu1—O7	91.72 (6)
O3—Cu1—O5	169.21 (5)	O1—Cu1—O7	89.67 (6)
O6—Cu1—O5	90.04 (6)	O3—Cu1—Cu1^i	85.69 (4)
O3—Cu1—O1	88.91 (6)	O6—Cu1—Cu1^i	86.89 (4)
O6—Cu1—O1	169.03 (5)	O5—Cu1—Cu1^i	83.52 (4)
O5—Cu1—O1	89.93 (6)	O1—Cu1—Cu1^i	82.20 (4)
O3—Cu1—O7	98.99 (6)	O7—Cu1—Cu1^i	170.56 (5)
O6—Cu1—O7	101.30 (6)		

Symmetry code i = 1 − x,1 − y,1 − z.

hydroxy-6-isopropyl-3-methylbenzoic acid) (HDCA) **2**, a derivative of carvacrol **3**, to evaluate its antibacterial and antiproliferative activities. To our knowledge, this type of metal complex obtained from a derivative of this natural product is the first example reported in the literature as well as their antimicrobial and antiproliferative activity studies.

The overall aim of this study was to develop a new and unknown type of copper(II) complexes with that derivative of the natural product carvacrol, to test their antimicrobial and antiproliferative activities and compare them with those of carvacrol.

2. Experimental

2.1. General materials and procedures for the synthesis of the complex

The synthetic work was performed in air. Commercially available reagents and solvents were used as received, without further purification or drying. $Cu(NO_3)_2{\cdot}2.5H_2O$ was used for the synthesis of complex **1**.

C, H, and N elemental analysis was carried out by the Microanalytical Service of the Instituto Superior Técnico. Infrared spectra (4000–400 cm^{-1}) were recorded on a Bruker Vertex 70 instrument in KBr pellets; wavenumbers are in cm^{-1}. Mass spectrum of **1** was run in a Varian 500-MS LC Ion Trap Mass Spectrometer equipped with an electrospray (ESI) ion source. For electrospray ionization, the drying gas and flow rate were optimized according to the particular sample with 35 p.s.i. nebulizer pressure. Scanning was performed from m/z 100 to 1200 in ethanol solution. The compound was observed in the positive mode (capillary voltage = 80–105 V).

2.2. Synthesis of $[Cu(DCA)_2(EtOH)]_2{\cdot}2EtOH$ (1)

0.390 g (2.0 mmol) of *O*-carvacrotinic acid (DCA) **2** was dissolved in 15 mL ethanol, and 10 mL of an aqueous solution of $Cu(NO_3)_2{\cdot}2.5H_2O$ (0.245 g, 1.05 mmol) were added to it. The resultant mixture was stirred at 50 °C for 15 min to obtain a green solution. The mixture was then filtered, and the solvent was evaporated slowly. After 3–4 days, single crystals suitable for X-ray diffraction were isolated, washed 2 times with cold ethanol-water mixture and dried in open air.

Yield: 0.412 g (76%, with respect to Cu(II)). Anal. Calcd for (**1**) $C_{52}H_{76}Cu_2O_{16}$: C, 57.60; H, 7.07. Found: C, 57.52; H, 7.02. IR (KBr; cm^{-1}): 3461 ν(OH), 1611 ν_{as}(COO$^-$), 1407 ν_s(COO$^-$). ESI-MS (+): m/z 588 [M/2 + (EtOH) + H] $^+$ (100%).

2.3. X-ray measurements

A good quality single crystal suitable for X-ray diffraction of **1** was immersed in cryo-oil, mounted in Nylon loops and measured at a temperature of 150 K. Intensity data were collected using a Bruker AXS PHOTON 100 diffractometer with graphite monochromated Mo-Kα (λ 0.71073) radiation. Data were collected using omega scans of 0.5° per frame and full sphere of data were obtained. Cell parameters were retrieved using Bruker SMART [23] software and refined using Bruker SAINT [23] on all the observed reflections. Absorption corrections were applied using SADABS [24]. Structures were solved by direct methods by using SIR97 [25] and refined with SHELXL2014 [26]. Calculations were performed using WinGX v2014.1 [27]. All non-hydrogen atoms were refined anisotropically. Those H-atoms bonded to carbon were included in the model at geometrically calculated positions and refined

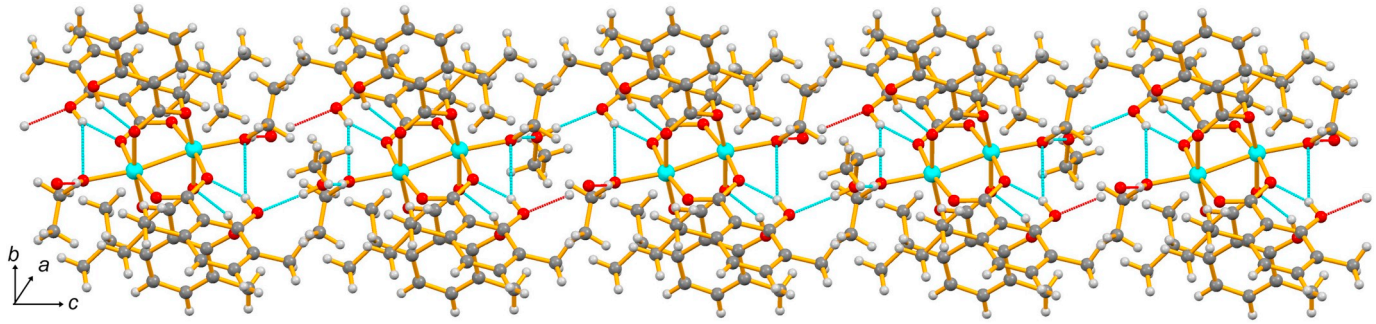

Fig. 2. Hydrogen bonded 1D supramolecular structure of **1** (along c-axis).

Table 3
MIC and MBC (or MFC) values of the compounds obtained by the microdilution method* against Gram-negative and Gram-positive bacteria and yeasts strains in μg/mL.

	S. aureus		*E. faecalis*		*P. aeruginosa*		*E. coli*		*C. albicans*		*S. cereviseae*	
Compound	MIC	MBC	MIC	MBC	MIC	MBC	MIC	MBC	MIC	MBC	MIC	MBC
Complex **1**	> 125	> 500	> 125	> 500	> 125	> 500	125	> 500	> 62.5	> 62.5	> 125	> 125
HDCA **2**	> 125	> 500	> 125	> 500	> 125	> 500	125	> 500	> 62.5	> 62.5	> 125	> 125
Positive control	7.82 VAN	nt	1.95	nt	< 0.48 NOR	nt	0.98	nt	< 0.48 NYS	nt	< 0.48	nt

nt– not tested; VAN – Vancomycin; NOR – Norfloxacin; NYS – Nystatin.
Results represent a median of at least three independent experiments.

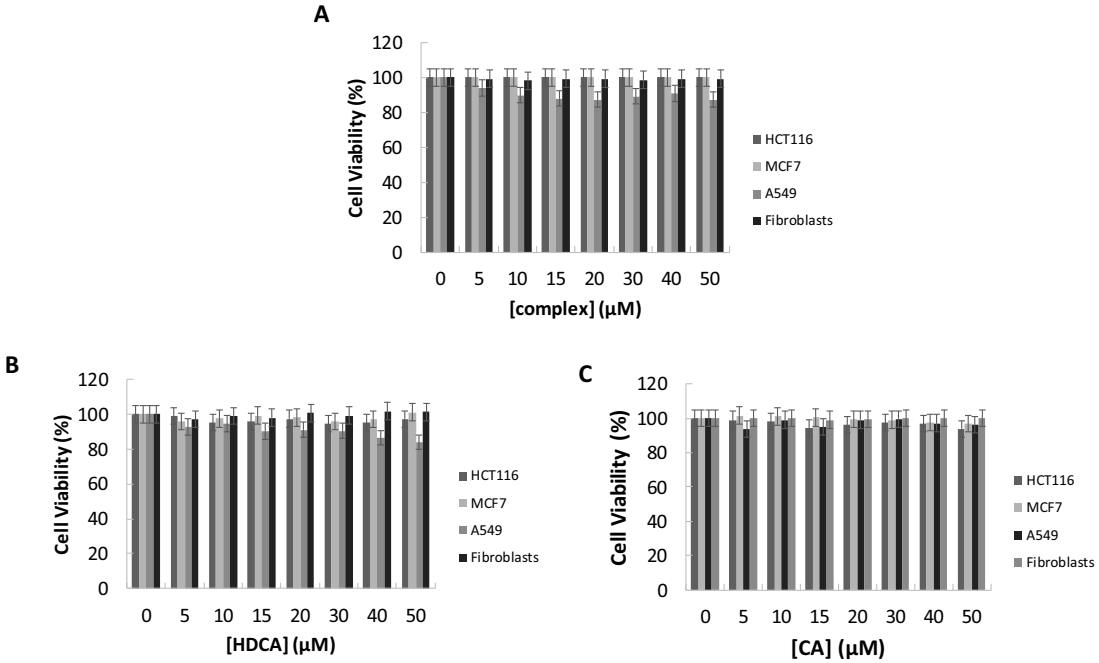

Fig. 3. Cytotoxicity of complex **1**, *O*-carvacrotinic acid (HDCA) **2** and carvacrol (CA) **3** and in HCT116, A549, MCF7 tumor cell lines and in normal primary human fibroblasts. Fibroblasts (black bars), HCT116 cells (dark grey bars), A549 (medium grey bars), MCF7 (light grey bars) cells were treated with increasing concentrations of the complex **1** (A), HDCA **2** (B) and CA **3** (C) for 48 h and cell viability was determined by MTS assay. The data were normalized against the control treated with 0.1% (v/v) DMSO. The results showed are expressed as mean ± SEM of three independent assays.

using a riding model. $U_{iso}(H)$ were defined as $1.2U_{eq}$ of the parent carbon atoms for phenyl and methyne residues and $1.5U_{eq}$ of the parent carbon atoms for the methyl groups. The other hydrogen atoms (O—H and N—H) were located in the difference Fourier synthesis and refined. Least square refinements with anisotropic thermal motion parameters for all the non-hydrogen atoms and isotropic for the remaining atoms were employed.

2.4. Biological assays

2.4.1. Cell culture

Human colorectal carcinoma (HCT116), lung adenocarcinoma (A549) and ovarian carcinoma (A2780) cell lines were grown in Dulbecco's modified Eagle's medium (DMEM) (Invitrogen Corp., Grand Island, NY, USA) supplemented with 10% foetal bovine serum and 1% antibiotic/antimycotic solution (Invitrogen Corp.) and maintained at 37 °C in a humidified atmosphere of 5% (v/v) CO_2 [28–30]. MCF7 cell line was grown in similar conditions, supplemented with 1% MEM non-essential amino acids (Invitrogen Corp.) [28]. Normal primary human fibroblasts were grown in the same conditions as MCF7 cell line [28–30]. All cell lines were purchase from ATCC (www.atcc.org).

2.4.1.1. Complexes exposure for dose-response curves. Cells were plated at 5000 cells/well in 96-well plates. Media was removed 24 h after platting and replaced with fresh media containing 0.1–50 μM of complex **1**, *O*-carvacrotinic acid (HDCA) **2** and carvacrol (CA) **3** or 0.1% (v/v) DMSO (vehicle control) for all cell lines, except for A2780, that a range between 0.1 and 150 μM of complex **1**, *O*-carvacrotinic acid (HDCA) **2** and carvacrol (CA) **3** was tested. All the previous solutions were prepared from concentrated stock solutions (in DMSO) of the complex, HDCA and CA.

2.4.1.2. Cytotoxicity. After 48 h of cell incubation in the presence or absence of compounds, cell viability was evaluated with CellTiter 96® AQueous Non-Radioactive Cell Proliferation Assay (Promega, Madison, WI, USA), using 3-(4,5-dimethylthiazol-2-yl)-5-(3-carboxymethoxyphenyl) -2-(4-sulfophenyl)-2H-tetrazolium, inner salt (MTS) as previously described [31,32]. The conversion of MTS into the aqueous soluble formazan product is accomplished by dehydrogenase enzymes found in metabolically active cells. The quantity of formazan product was measured in a Bio-Rad microplate reader Model 680 (Bio-Rad, Hercules, CA, USA) at 490 nm, as absorbance is directly proportional to the number of viable cells in culture.

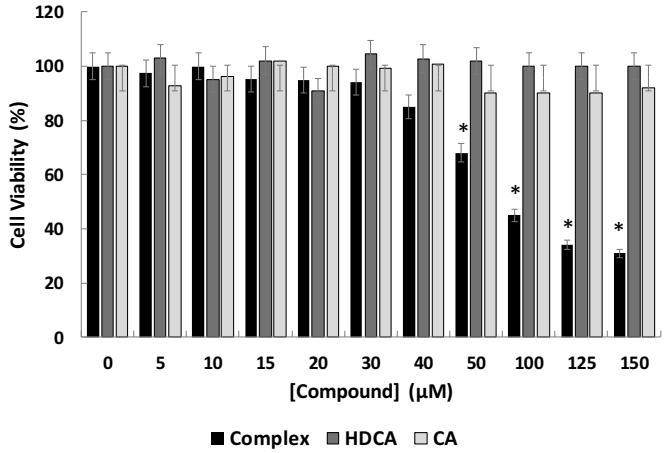

Fig. 4. Cytotoxicity of complex **1**, HDCA **2** and CA **3** in A2780 tumor cell line. A2780 cells were treated with increasing concentrations of the complex for 48 h and cell viability was determined by MTS assay. Data were normalized against the control (0.1% (v/v) DMSO). The results showed are expressed as mean ± SEM of three independent assays. The symbol * in the figure means that the results are statistically significant with a $p < 0.05$ (as compared control).

2.4.1.3. Apoptosis via Hoechst staining. A2780 cells grown as described above were plated at 7500 cells/mL and incubated for 48 h in culture medium containing the complex **1** or 0.1% (v/v) DMSO (vehicle control). Hoechst staining was used to detect apoptotic nuclei as previously described [33]. Briefly, after removal of cell medium, cells were washed with phosphate-buffered saline (PBS) 1× (Invitrogen), fixed with paraformaldehyde (4% (v/v); in PBS 1×) for 10 min in the dark and incubated with Hoechst 33258 (5 μg/mL in PBS 1×; Sigma, Missouri, USA) for an additional 10 min. Cell were washed with PBS 1× and mounted using 20 μL of PBS:glicerol (3:1; v/v) solution. Fluorescent nuclei were sort out according to the chromatin condensation degree and characteristics. Normal nuclei presented non-condensed chromatin uniformly distributed over the entire nucleus and apoptotic nuclei showed condensate or fragmented chromatin. Some apoptotic cells formed apoptotic bodies. Plates were photographed in an AXIO Scope (Carl Zeiss, Oberkochen Germany), and three random microscopic fields per sample with ca. 50 nuclei were counted. Mean values were expressed as the percentage of apoptotic nuclei [33].

2.4.1.4. Statistical analysis. All data were expressed as mean ± SEM from at least three independent experiments. Statistical significance was evaluated using the Student's *t*-test; $p < 0.05$ was considered statistically significant.

2.4.2. Microorganisms - antimicrobial assays - determination of MIC and MBC

The Gram-positive and negative bacteria used throughout this study were *Enterococcus faecalis* (ATCC 29212), *Pseudomonas aeruginosa* (ATCC 27853), *Escherichia coli* (ATCC 25922) and *Staphylococcus aureus* (ATCC 25923), respectively. The yeasts in this study were *Candida albicans* ATCC 10231 and *Saccharomyces cerevisiae* (ATCC 9763).

Under aseptic conditions, 100 μL of broth medium was distributed in each well of a 96-well plate. Mueller-Hinton and Sabouraud broth were used for bacteria or yeasts, respectively. To the first well of each row was added 100 μL of the interest compound at a concentration of 1 mg/mL, Positive control solutions (vancomycin, norfloxacin and nystatin) with the same concentration were prepared and DMSO was used as negative control. Afterwards, 1:2 microdilution series was made and 10 μL of bacterial suspension at 0.5 McFarland concentration were added to each well. Incubation of the plates at 37 °C for 24 h allowed the microbial growth, and after that period the plates were analysed.

To perform the MBC assay, a swab from MIC wells was spread on the surface of agar medium - previously inoculated with the correspondent microorganism. After 24 h incubation at 37 °C, the lowest concentration that revealed no visible microbial growth was taken as its MBC. All assays were carried out in triplicate for each tested microorganism.

3. Results and discussion

The reaction of *O*-carvacrotinic acid (2-hydroxy-6-isopropyl-3-methylbenzoic acid) (HDCA) **2** with $Cu(NO_3)_2{\cdot}2.5H_2O$ in ethanol-water medium results in the formation of the dinuclear Cu(II) complex $[Cu(DCA)_2(EtOH)]_2{\cdot}2EtOH$ (**1**) (Scheme 1).

The characterization of complex **1** has been carried out by elemental analysis, IR spectroscopy, ESI-MS and single crystal X-ray diffraction techniques. The IR spectrum of complex **1** displays the O—H absorption band of ethanol molecule at 3461 cm^{-1}. The presence of intramolecular hydrogen bond systems is observed in the region 3000–2600 cm^{-1}. The antisymmetric and symmetric COO^- vibration at 1611 and 1407 cm^{-1} supports the presence of carboxylate bonding in complex **1** [34]. In the ESI-MS spectrum, the *m/z* value of complex **1** indicates the decomposition of the binuclear species to a mononuclear unit in solution (see Experimental). The X-ray crystal structure is described below, as well as the antibacterial and antiproliferative activities of the dinuclear Cu(II) complex **1**, the free *O*-carvacrotinic acid (HDCA) **2** and the natural product carvacrol **3**.

3.1. X-ray structure

X-ray quality crystals of complex **1** were obtained upon slow evaporation, at room temperature, of water-ethanol mixture of the compound. Complex **1** crystallizes in the triclinic $P\bar{1}$ space group with an

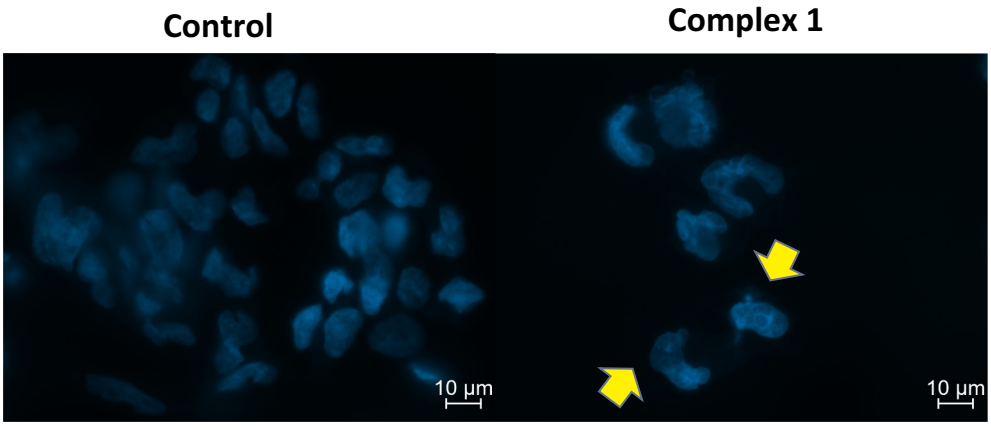

Fig. 5. - Apoptotic morphological changes in A2780 cells exposed to 0.1% DMSO (control) or complex **1**. Cells were treated the IC_{50} of the complex **1** for 48 h and stained with Hoechst 33258. Typical morphologic features of apoptosis like chromatin condensation and apoptotic bodies formation (arrows) were identified in the presence of the complex **1**.

inversion centre located between the copper ions of dinuclear paddle-wheel centrosymmetric molecule. The molecular structure of complex **1** is presented in Fig. 1, crystallographic data and processing parameters are summarized in Table 1 and selected dimensions in Table 2. Four *O*-carvacrotinate ligands and two ethanol molecules surround the two Cu (II) atoms. Each copper atom is connected to four oxygen atoms from the carboxylate ligands, which form a square plane, and to one oxygen atom of ethanol ligand placed at the apical position. The Cu—Cu distance is 2.5959 (4) Å. The copper centre is therefore considered as square pyramidal, neglecting the Cu—Cu interaction with τ_5 value of 0.003. The bond lengths and angles observed are very similar with no significant deviations from those previously reported [34]. The Cu atom lies 0.186 Å from this plane in the axial direction towards the ethanol molecule. There are two non-coordinated ethanol molecules in the structure involved in hydrogen bonding to form a 1D supramolecular chain (Fig. 2).

3.2. Antimicrobial assays

As can be observed in Table 3, MIC ranged between values greater than 62.5 and 125 μg/mL, thus indicating that complex **1** and its free pro-ligand *O*-carvacrotinic acid (HDCA) **2** do not show significant antimicrobial activity. However, overall both compounds showed to be more effective on yeasts rather than on bacteria, with lower MIC and MBC values. Regarding to bacteria activity, the MBC to MIC ratio is greater than four indicating that the compounds appear to present a bacteriostatic behaviour, rather than a bactericide one.

3.3. Antiproliferative assays

The cytotoxic activities of the complex **1**, the pro-ligand *O*-carvacrotinic acid (HDCA) **2** and carvacrol (CA) **3** were assessed by the MTS assay on representative human cancer cell lines: ovarian carcinoma (A2780), colorectal carcinoma (HCT116), breast adenocarcinoma (MCF7) and lung adenocarcinoma (A549) and in normal human primary fibroblasts (Figs. 3–4).

No cytotoxic activity is observed after the incubation with the complex **1**, *O*-carvacrotinic acid (HDCA) **2** and carvacrol (CA) **3** in HCT116, A459, MCF7 cancer cell lines (Fig. 3) (IC_{50} higher than 50 μM) except for A2780 that presents an IC_{50} of 54 ± 0.2 μM (Fig. 4). Indeed, A2780 cell line seems to be more sensitive to the presence of HDCA, CA or the complex in comparison to the other cancer cell lines studied (HCT116, MCF7 and A549) (Figs. 3–4). Importantly, the complex **1**, *O*-carvacrotinic acid (HDCA) **2** and carvacrol (CA) **3** have no cytotoxic activity in normal primary human (Fig. 3) which reinforces its selectivity towards ovarian carcinoma cells (Fig. 4).

The moderate reduction of cell viability promoted by complex **1** in A2780 cells (Fig. 4) prompted us to evaluate the underlined mechanisms of cell death. A preliminary analysis with Hoechst 33258 dye allows the detection of nuclear alterations like chromatin condensation and nuclear fragmentation, typical features of apoptotic cells [35]. Hoechst 33258 staining of A2780 cells after 48 h of exposure to the IC_{50} of complex **1** allowed us to observe a reduction in the number of stained cells compared to control cells and the nuclear condensation and apoptotic bodies formation characteristics of apoptosis (Fig. 5).

When we compare our complex **1** with other natural products derivatives in terms of biological activity (e.g. copper(II) complex with N-(pyridin-2-ylmethylene) dehydroabietylamine as ligand [36]) the later IC_{50} is much lower but both induce tumor cells apoptosis. When we compare to curcumin metal derivatives while free curcumin induces 50% of cytotoxicity (IC_{50}) at concentrations < 10 μM, the zinc(II) complexes are, however, less cytotoxic (IC_{50} = 12–37 μM) in prostate cancer cells [37]. In our case, complex **1** is more active at least in A2780 cells compared to free ligand.

4. Conclusions

In this study, the synthesis and characterization of a novel dinuclear Cu(II) complex **1** derived from *O*-carvacrotinic acid **2** is reported for the first time. Our aim was to explore the antibacterial and antiproliferative potential of this complex and of *O*-carvacrotinic acid **2,** a derivative of the natural product carvacrol **3** (well known as a strong antimicrobial and antitumoral potential). The tested compounds show less antimicrobial activity than carvacrol. Nevertheless, the analysis of their MBC to MIC ratio suggests that their behaviour seems to be bacteriostatic, rather than bactericide. Overall, a better activity was observed on yeasts, especially against *C. albicans*, thus showing potential interest in topical applications.

The antiproliferative potential of complex **1**, carvacrotinic acid (HDCA) **2** and carvacrol (CA) **3** was examined towards A2780 human ovarian carcinoma, HCT116 colorectal carcinoma, A549 lung adenocarcinoma and MCF7 breast adenocarcinoma cell lines. The complex **1**, HDCA **2** and CA **3** were found to have no antiproliferative effect on HCT116, A549 and MCF7 tumor cell lines. However, the complex shows a moderate activity towards A2780 ovarian carcinoma cell line compared to HDCA **2** and CA **3**. The moderate viability loss induced by complex **1** agreed with Hoechst 33258 staining and the typical morphological apoptotic characteristics like chromatin condensation and apoptotic bodies formation. Taken together, these results demonstrate that in comparison to HDCA **2** and CA **3**, the complex **1** provides several advantages namely its higher cytotoxic potential in A2780 cell line with the simultaneously no cytotoxicity in healthy cells (up to 50 μM), making this a positive feature for further development particularly towards ovarian carcinoma.

Further studies are undergoing in our laboratory for the synthesis of new series of complexes with other natural product ligands and metals.

Acknowledgements

Authors are grateful to the Fundação para a Ciência e a Tecnologia (FCT) (projects PTDC/EQU-EQU/122025/2010 and UID/QUI/00100/2013), Portugal, for financial support. M.S. acknowledges the FCT, Portugal for a postdoctoral fellowship (SFRH/BPD/86067/2012). This work was supported by the Unidade de Ciências Biomoleculares Aplicadas - UCIBIO which is financed by national funds from FCT/MEC (UID/Multi/04378/2013) and co-financed by the ERDF under the PT2020 Partnership Agreement (POCI-01-0145-FEDER-007728). P*V* Baptista is acknowledged for access to microplate reader and inverted microscope.

Appendix A. Supplementary data

CCDC 1830895 for **1** contains the supplementary crystallographic data for this paper. This data can be obtained free of charge from The Cambridge Crystallographic Data Centre via www.ccdc.cam.ac.uk/data_request/cif. Supplementary data to this article can be found online at https://doi.org/10.1016/j.jinorgbio.2018.09.018.

References

[1] A. Guarda, J.F. Rubilar, J. Miltz, M.J. Galotto, Int. J. Food Microbiol. 146 (2011) 144–150.
[2] F. Chen, Z. Shi, K.G. Neoh, E.T. Kang, Biotechnol. Bioeng. 104 (2009) 30–39.
[3] K. Husnu Can Baser, Curr. Pharm. Des. 14 (2008) 3106–3120.
[4] A. Nostro, R. Scaffaro, M. D'Arrigo, L. Botta, A. Filocamo, A. Marino, G. Bisignano, Appl. Microbiol. Biotechnol. 96 (2012) 1029–1038.
[5] A.B. Arfa, Y. Chrakabandhu, L. Preziosi-Belloy, P. Chalier, N. Gontard, Food Res. Int. 40 (2007) 22–32.
[6] M.L. Arrebola, M.C. Navarro, J. Jiménez, F.A. Ocaña, Phytochemistry 36 (1994) 67–72.
[7] M. Sökmen, J. Serkedjieva, D. Daferera, M. Gulluce, M. Polissiou, B. Tepe, H.A. Akpulat, F. Sahin, A. Sökmen, J. Agric. Food Chem. 52 (2004) 3309–3312.
[8] H.J. Dorman, S.G. Deans, J. Appl. Microbiol. 88 (2000) 308–316.
[9] M. Friedman, P.R. Henika, R.E. Mandrell, J. Food Prot. 65 (2002) 1545–1560.

[10] E.J.A. Veldhuizen, J.L.M. Tjeerdsma-Van Bokhoven, C. Zweijtzer, S.A. Burt, H.P. Haagsman, J. Agric. Food Chem. 54 (2006) 1874–1879.
[11] W. Dai, C. Sun, S. Huang, Q. Zhou, Onco Targets Ther. 9 (2016) 2297–2304.
[12] K. Fan, X. Li, Y. Cao, H. Qi, L. Li, Q. Zhang, H. Sun, Anti-Cancer Drugs (8) (2015) 813–823.
[13] Q.H. Yin, F.X. Yan, X.Y. Zu, Y.H. Wu, X.P. Wu, M.C. Liao, S.W. Deng, L.L. Yin, Y.Z. Zhuang, Cytotechnology 64 (2012) 43–51.
[14] A. Nostro, T. Papalia, Recent Pat Antiinfect Drug Discov. 7 (2012) 28–35.
[15] Z.E. Suntres, J. Coccimiglio, M. Alipour, Crit. Rev. Food Sci. Nutr. 55 (2015) 304–318.
[16] B. de Las Heras, A. Amesty, A. Estevez-Braun, S. Hortelano, Anti Cancer Agents Med. Chem. (2018), https://doi.org/10.2174/1871520618666180420165821.
[17] A.L. Picciano, T.D. Vaden, Biophys. Chem. 184 (2013) 62–67.
[18] B. A Barik, A. Mishra, R.M. Kunwar, L. Kadam, S. Shen, S. Dutta, A.K. Padhye, H.Y. Satpati, K. Zhang, Indira Priyadarsini, Eur. J. Med. Chem. 42 (2007) 431–439.
[19] R. Banerjee, Bioinorg. Chem. Appl. 2014 (2014) (Artice ID 325873).
[20] D.J. Newman, G.M. Cragg, J. Nat. Prod. 79 (2016) 629–661.
[21] E. Ferrari, R. Benassi, M. Saladini, G. Orteca, Z. Gazova, K. Siposova, Chem. Biol. Drug Des. 89 (2017) 411–419.
[22] F.S. Yan, J.L. Sun, W.H. Xie, L. Shen, H.F. Ji, Nutrients 10 (28) (2017) 1–11.
[23] Bruker, APEX2, Bruker AXS Inc, Madison, Wisconsin, USA, 2012.
[24] G.M. Sheldrick, SADABS. Program for Empirical Absorption Correction, University of Gottingen, Germany, 1996.
[25] A. Altomare, M.C. Burla, M. Camalli, G.L. Cascarano, C. Giacovazzo, A. Guagliardi, A.G.G. Moliterni, G. Polidori, R. Spagna, J. Appl. Crystallogr. 32 (1999) 115–119.
[26] G.M. Sheldrick, A short history of SHELX, Acta Crystallogr. A 64 (2008) 112–122.
[27] L.J. Farrugia, J. Appl. Crystallogr. 45 (2012) 849–854.
[28] T.F.S. Silva, P. Smoleński, L.M.D.R.S. Martins, M.F.C. Guedes Da Silva, A.R. Fernandes, D. Luis, A. Silva, S. Santos, P.M. Borralho, C.M.P. Rodrigues, A.J.L. Pombeiro, Eur. J. Inorg. Chem. (2013) 3651–3658.
[29] A. Silva, D. Luis, S. Santos, J. Silva, A.S. Mendo, L. Coito, T.F. Silva, M.F. da Silva, L.M. Martins, A.J. Pombeiro, P.M. Borralho, C.M. Rodrigues, M.G. Cabral, P.A. Videira, C. Monteiro, A.F. Fernandes, Drug Metabol. Drug Interact. 28 (2013) 167–176.
[30] T.F.S. Silva, L.M.D.R.S. Martins, M.F.C. Guedes Da Silva, A.R. Fernandes, A. Silva, P.M. Borralho, S. Santos, C.M.P. Rodrigues, A.J.L. Pombeiro, Dalton Trans. 41 (2012) 12888–12897.
[31] L.R. Raposo, C. Roma-Rodrigues, J. Jesus, L.M.D.R.S. Martins, A.J.L. Pombeiro, P.V. Baptista, A.R. Fernandes, Vet. Comp. Oncol. (2017) 1–6.
[32] O.A. Lenis-Rojas, A.R. Fernandes, C. Rodrigues, P.V. Baptista, F.M. Marques, D. Pérez-Fernández, J. Guerra, L.E. Sanchez, D. Vazquez-Garcia, M. Lopez-Torres, A. Fernández, J.J. Fernández Sánchez, Dalton Trans. 45 (2016) 19127–19140.
[33] M. Sutradhar Rajeshwari, T. Roy Barman, A.R. Fernandes, F. Paradinha, C. Roma-Rodrigues, M.F.C. Guedes da Silva, A.J.L. Pombeiro, J. Inorg. Biochem. 175 (2017) 267–275.
[34] M. Puchoňová, M. Mazúr, J. Moncol, Z. Růžičková, D. Valigura, J. Mol. Struct. 1137 (2017) 706–713.
[35] S.A. O'Toole, B.L. Sheppard, E.P.J. McGuinness, N.C. Gleeson, M. Yoneda, J. Bonnar, Cancer Detect. Prev. 27 (2003) 47–54.
[36] B.L. Fei, B. Yin, D.D. Li, W.S. Xu, Y. Lu, J. Biol. Inorg. Chem. 21 (2016) 987–996.
[37] D. Pucci, A. Crispini, B.S. Mendiguchía, S. Pirillo, M. Ghedini, S. Morellib, L.D. Bartolob, Dalton Trans. 42 (2013) 9679–9687.